Effects of atmospheric inorganic nitrogen deposition on ocean biogeochemistry

Aparna Krishnamurthy,[1] J. Keith Moore,[1] Charles S. Zender,[1] and Chao Luo[1]

Received 2 October 2006; revised 2 February 2007; accepted 7 March 2007; published 9 May 2007.

[1] We perform a sensitivity study with the Biogeochemical Elemental Cycling (BEC) ocean model to understand the impact of atmospheric inorganic nitrogen deposition on marine biogeochemistry and air-sea CO_2 exchange. Simulations involved examining the response to three different atmospheric inorganic nitrogen deposition scenarios namely, Pre-industrial (22 Tg N/year), 1990s (39 Tg N/year), and an Intergovernmental Panel on Climate Change (IPCC) prediction for 2100, IPCC-A1FI (69 Tg N/year). Globally, the increasing N deposition had widespread, but modest effects on export production and air-sea CO_2 exchange. The maximum increase in N deposition was 47 Tg N/year since Pre-industrial control for the IPCC-A1FI case, which had an increase in primary production (0.98 Gt C/year or 2%), export production (0.16 Gt C/year or 3%) and a decrease in atmospheric pCO_2 of 1.66 ppm (0.6%) relative to the Pre-industrial control. In some regions, atmospheric N inputs supported >20% of the export production in the current era and >50% of the export production in the IPCC-A1FI case. As nitrogen deposition increased, N fixation decreased because the diazotrophs were outcompeted by diatoms and small phytoplankton under more N-replete conditions. This decrease in N fixation could partially counteract the ongoing increase in new nitrogen inputs via atmospheric N deposition.

Citation: Krishnamurthy, A., J. K. Moore, C. S. Zender, and C. Luo (2007), Effects of atmospheric inorganic nitrogen deposition on ocean biogeochemistry, *J. Geophys. Res.*, *112*, G02019, doi:10.1029/2006JG000334.

1. Introduction

[2] Marine biological production in the presence of nutrients is one of the key factors that control the strength of the oceanic biological carbon pump hence impacting the atmospheric partial pressure of carbon dioxide (pCO_2) [*Gruber*, 2004]. Production by phytoplankton occurs in the presence of light and critical nutrients, such as nitrogen, phosphorous, silicon and iron. These nutrients are obtained from upwelling and entrainment of subsurface waters, riverine inputs and by atmospheric deposition. In the last few decades the important role of atmospheric deposition of nutrients over oceans has been well established and in many areas they have been found to exceed riverine inputs [*Duce*, 1986]. In some regions, the atmosphere provides a vital transport path for nitrogen and iron [*Duce et al.*, 1991]. Past studies have also suggested that atmospheric nitrogen was quantitatively an important source of external or "new" nitrogen to many geographically diverse marine and freshwater ecosystems [*Paerl*, 1993, 1995; *Jassby et al.*, 1994].

[3] Inorganic nitrogen (ammonia and nitrate) sources include fossil fuel combustion [*Hameed and Dignon*, 1988], biomass burning, soil emissions and breakdown of urea from domestic animals [*Warneck*, 1988]. *Jickells* [2005] suggested that atmospheric inorganic nitrogen is emitted naturally via ammonia and nitrous oxide from soils, plants and animal wastes. On a global scale, atmospheric deposition of inorganic nitrogen in oxidized (nitrate) and reduced (ammonia) forms dominate nitrogen inputs into oceans [*Paerl and Whittal*, 1999]. Occurrences of large episodic events of atmospheric nitrogen inputs can strongly impact the surface ocean biogeochemistry [*Paerl*, 1985]. Current estimates of atmospheric nitrogen inputs into oceans constitute primarily the inorganic nitrogen although more than half of the fluvial inputs of dissolved fixed nitrogen is dissolved organic nitrogen [*Cornell et al.*, 1995]. On the basis of their study, *Cornell et al.* [1995] found that precipitation in the form of rain and snow can also be an important source of organic nitrogen to oceans.

[4] Nitrogen species that can be utilized as nutrients by marine organisms are of two types namely, oxidized nitrogen species that include aerosol nitrate (NO_3^-) and gas phase oxides of nitrogen (NO, NO_2, HNO_3 and related species) and reduced nitrogen species that include aerosol NH_4^+ and gaseous NH_3 (and related organic nitrogen species) [*Duce et al.*, 1991]. The largest anthropogenic source of NO_x is fossil fuel combustion followed by biomass burning [*Logan*, 1983; *Hameed and Dignon*, 1988, *Crutzen*, 1990]. The major natural atmospheric source of NO is lightning [*Duce et al.*, 1991]. Important sources of reduced nitrogen are domestic animals, soil emissions and biomass burning [*Warneck*, 1988].

[1]Earth System Science Department, University of California, Irvine, California, USA.

0148-0227/07/2006JG000334

[5] Nitrogen oxides and dioxides collectively summed up as NO_x gets oxidized to nitric acid that can directly deposit or react with alkaline atmospheric aerosols [*Jickells*, 2005]. These aerosols can be removed by wet and dry deposition. Many studies have determined that substantial modifications can occur to aerosol particle size and deposition rates owing to reactions between nitric acid and seasalt [*Jickells*, 1998; *De Leeuw et al.*, 2001; *Paerl et al.*, 2002; *Pryor and Sorensen*, 2002].

[6] Anthropogenic activities have increased nitrogen emissions from land to the atmosphere. This has almost doubled globally with much bigger increase in some regions [*Prospero et al.*, 1996; *Galloway and Cowling*, 2002; *Jickells*, 2002]. Increased new nitrogen loading to geographically diverse marine and freshwater ecosystems has led to widespread coastal eutrophication, as a result of increased biological production [*Paerl*, 1993, 1995; *Jassby et al.*, 1994; *Nixon*, 1995]. Recent studies have concluded that atmospheric concentrations of combined nitrogen species will rise globally owing to increased combustion of fossil fuel and fertilizer use [*Galloway*, 1995; *Prospero et al.*, 1996]. *Galloway* [1995] suggested that emissions in the developing regions of the world, especially Asia is likely to increase and exceed the combined emissions of North America and Europe by 2020. *Luo et al.* [2007] used an inorganic aerosol thermodynamic equilibrium model coupled to a three-dimensional chemical transport model to estimate the impact of ammonia chemistry and natural aerosols on the global distribution of aerosols. Their study concluded that current atmospheric NO_3 and NH_4 deposition values are twice the values during Pre-industrial conditions. Their N deposition estimates are used in this study.

[7] Previous studies have estimated regional impacts of atmospheric deposition of nitrogen on oceanic ecosystem and biogeochemistry. In a study at coastal North Carolina, *Paerl* [1985] found that continentally fed acidic rainfall contained more inorganic nitrogen in the form of nitrate, nitrite and ammonia than near neutral rainfall resulting from oceanic fronts. He concluded that, the more acidic the rain, the higher the inorganic nitrogen inputs and the associated phytoplankton bloom. *Spokes et al.* [2000] did a study during May 1997 over Atlantic Ocean off the coast of Ireland. They found that short-duration south easterly transport events brought high concentrations of nitrogen. These deposition events were associated with air mass from polluted regions of UK and northern Europe. These atmospheric inputs contributed to approximately 30% of the new production. Hence long-term human-induced environmental perturbations can influence the atmospheric inputs of nitrogen into the ocean. Land use changes, rapid urbanization, and increasing fossil fuel emissions will affect the nutrient deposition over global oceans.

[8] The Biogeochemical Elemental Cycling model (BEC) used in this study was recently used to examine changes in dust/iron deposition over decadal timescales using dust estimates from Last Glacial Maximum (LGM), Pre-industrial, current (1990s) and future era (CO_2 double Pre-industrial values) [*Moore et al.*, 2006]. Their study found significant impacts on nitrogen fixation and sinking carbon export at various regions of the world ocean, leading to changes in global air-sea CO_2 exchange. Another recent study using the BEC model quantified the key role played by atmospheric iron inputs in driving marine nitrogen fixation and denitrification [*Moore and Doney*, 2007]. This study also found significant influence of surface water inorganic N/P ratios on global N fixation rates.

[9] This paper describes a sensitivity study with the BEC model to simulate the oceanic biogeochemical impacts of three different atmospheric inorganic nitrogen deposition scenarios, namely Pre-industrial (low), during 1990s (intermediate), and an Intergovernmental Panel for Climate Change (IPCC) prediction for 2100 (A1FI) (high). Sixty-four-year-long simulations were performed to understand the influence of the low, intermediate and high atmospheric N inputs on the marine ecosystem. Global estimates of nitrogen fixation, sinking particulate organic export (POC) at 103 m and air-sea CO_2 flux were calculated. The amount of sinking particulate organic nitrogen (PON) export potentially driven by atmospheric N deposition was also estimated. Across the global oceans, the effects of increased atmospheric N inputs resulted in a small increase in export production and air-sea CO_2 exchange. On a regional scale, atmospheric N inputs supported >20% of the export production under intermediate inorganic N inputs and >50% of the export production under high inorganic N inputs. There was also a decrease in nitrogen fixation as diazotroph growth was inhibited by competition with the diatom and small phytoplankton groups. This decrease in N fixation partially negates the effect of increasing new N inputs from atmospheric deposition.

2. Methods

[10] Simulations involved examining the marine ecosystem response to three different atmospheric inorganic nitrogen deposition scenarios namely, Pre-industrial, during the 1990s, and an Intergovernmental Panel for Climate Change (IPCC) predictions for 2100 (IPCC-A1FI). This fossil fuel intensive IPCC scenario was chosen to give a reasonable upper bound on N deposition [*Intergovernmental Panel for Climate Change*, 2000]. These predictions include a wide range of critical future characteristics such as demographic changes, economic development, and technological changes. The IPCC, A1FI is a fossil fuel intensive case, which assumes a future world with extensive reliance on fossil fuels. The effects on ocean biogeochemistry and air-sea CO_2 flux were simulated using the global Biogeochemical Elemental Cycling model (BEC) [*Moore et al.*, 2004]. The BEC model was run within the National Climate and Atmospheric Research's (NCAR) Community Climate System Model 3(CCSM) Parallel Ocean Program Ocean module [*Collins et al.*, 2006; *Yeager et al.*, 2006]. The resolution of the model is 3.6° longitude and 0.9°−2.0° latitude with the finer resolution near equator. The ecosystem component is coupled with a carbonate chemistry module based on the Ocean Carbon Model Intercomparison Project (OCMIP) [*Doney et al.*, 2003, 2004, 2006], allowing computation of surface ocean pCO_2 and air-sea CO_2 flux.

[11] The ecosystem module of the BEC model includes multiple growth limiting nutrients, nitrogen, phosphorus, iron and silicon. Two external iron sources, mineral dust and continental shelves, are also included [*Moore et al.*, 2002, 2004]. Iron binding ligands are not modeled explicitly but an iron scavenging parameterization based on ambient iron

Table 1. Parameter Changes in This Study Relative to *Moore et al.* [2004]

Parameter	Original Value	Modified Value	Units
alphaDiat	0.25	0.25	nmolC/cm^2/ngChlWday[a]
alphaSp	0.25	0.33	nmolC/cm^2/ngChlWday[b]
alphaDiaz	0.03	0.08	nmolC/cm2/ngChlWday[c]
graz_diat	1.2	1.25	mmol C[d]
thetaNmax_diat	3.0	4.0	mgChl/mmolN[e]
thetaNmax_sp	2.3	2.0	mgChl/mmolN[f]
thetaNmax_diaz	3.4	2.0	mgChl/mmolN[g]
diatom Kno3	2.5	1.5	μmol N[h]
diatom Knh4	0.08	0.05	μmol N[i]
diazotroph_Kfe	0.1	0.06	nM Fe[j]
Kdiazdop		0.025	μmol P[k]
Kspdop		0.25	μmol P[l]
umax_diat	2.07	2.25	per day[m]
dom remin rate	1/100	1/300	per day[n]
labile dom fraction	0.7	0.25	unitless[o]
f_graze_diat_doc	0.13	0.3	unitless[p]
f_graze_diaz_doc	0.24	0.4	unitless[q]
soft POM remin (where O2 < 4 μM)		390.0	m[r]

[a]Initial slope of P versus I curve for diatoms based on work by *Geider et al.* [1998] and Krishnamurthy et al. (submitted manuscript, 2007).
[b]Initial slope of P versus I curve for small phytoplankton based on work by *Geider et al.* [1998] and Krishnamurthy et al. (submitted manuscript, 2007).
[c]Initial slope of P versus I curve for diazotrophs based on work by *Geider et al.* [1998] and Krishnamurthy et al. (submitted manuscript, 2007).
[d]Grazing loss for diatoms.
[e]Maximum Chl/N ratio for diatoms based on work by *Geider et al.* [1998] and Krishnamurthy et al. (submitted manuscript, 2007).
[f]Maximum Chl/N ratio for small phytoplankton based on work by *Geider et al.* [1998] and Krishnamurthy et al. (submitted manuscript, 2007).
[g]Maximum Chl/N ratio for diazotrophs based on work by *Geider et al.* [1998] and Krishnamurthy et al. (submitted manuscript, 2007).
[h]Half saturation value for nitrate uptake by the diatoms.
[i]Half saturation value for ammonium uptake by the diatoms.
[j]Half saturation value for iron uptake by the diazotrophs.
[k]Half saturation value for P uptake from DOP for diazotrophs.
[l]Half saturation value for P uptake from DOP for small phytoplankton.
[m]Maximum grazing rate on diatoms.
[n]Remineralization rate of DOM.
[o]Fraction of labile DOM.
[p]Fraction of diatom grazing to DOC.
[q]Fraction of diazotroph grazing to DOC.
[r]Remineralization length scale under low O_2 conditions based on work by *Van Mooy et al.* [2002].

concentration and number of particles available to scavenge iron is used to account the effects of organic ligands [*Moore et al.*, 2004]. The biogeochemical cycling of carbon, nitrogen, phosphorus, silicon, oxygen, alkalinity and iron are simulated along with the growth of four phytoplankton functional groups. These are picoplankton, diatoms, diazotrophs and coccolithophores. Diazotrophs are parameterized to account for their higher N/P ratios (50 mol/mol), higher iron and light requirements and slower maximum growth rates. As the light and nutrient levels change, the model incorporates variable elemental ratios for C/Fe, C/Si, and C/Chlorophyll. The losses of the four phytoplankton species occurs via natural mortality, zooplankton grazing and phytoplankton aggregation. Detailed description of the model is available from *Moore et al.* [2002, 2004]. Certain parameters used in the original version of BEC model [*Moore et al.*, 2004] were modified to improve simulation results [*Moore et al.*, 2006] and these are summarized in Table 1. The initial slope of the P versus I curve, α and max. Chl/N ratios are based on work by A. Krishnamurthy et al. (The effects of dilution and mixed layer depth on deliberate ocean iron fertilization: 1-D simulations of the Southern Ocean Iron Experiment (SOFeX), submitted to *Journal of Marine Systems*, 2007) (hereinafter referred to as Krishnamurthy et al., submitted manuscript, 2007) (Table 1) and are closer to mean diatom versus nondiatom values from *Geider et al.* [1998].

[12] Water column denitrification under lower ambient oxygen concentrations is parameterized such that when O_2 concentrations fall below 4 μM, nitrate is consumed during remineralization of sinking particulate organic matter (POM) rather than O_2, with a stoichiometry of $117C16N1P + 120NO_3 => 117CO_2 + PO_4 + 68N_2$ [*Moore and Doney*, 2007]. The diazotrophs and small phytoplankton in these simulations are able to access dissolved organic phosphorus (DOP) as a source for phosphorus and we route a higher fraction of particulate organic matter (POM) to the semilabile dissolved organic pool when it is grazed. As the nutrient composition varies, the BEC model is able to reproduce the changes in community structure and biogeochemical rates, producing the observed ecosystem shifts from in situ iron fertilization experiments [*Moore et al.*, 2006; Krishnamurthy et al., submitted manuscript, 2007].

[13] The model has been validated by comparing with observed global-scale variations in primary and export production, biogenic silica production, calcification, and nitrogen fixation [see *Moore et al.*, 2002, 2004]. The BEC model has been spun up for three thousand years such that biogeochemical tracers are in quasi steady state with negligible drifts in key fluxes (air-sea CO_2 flux was 0.037 PgC/yr, and drifts in export and primary production over the last century were 0.0045%/century and 0.077%/century, respectively). The atmospheric pCO_2 was set to 278 ppm in this simulation. Iron inputs from dust and sedimentary sources were the only external nutrients. The model was spun up additionally for five hundred years with Pre-industrial N deposition. Then three 64-year simulations were conducted with the Pre-industrial, 1990s, and IPCC-A1FI nitrogen deposition scenarios. Atmospheric CO_2 estimations in the 500-year and follow on simulations were dynamic, such that atmospheric concentration was modeled as a single, well-mixed box in communication with the ocean. Monthly dust deposition data were obtained from *Zender et al.* [2003] assuming 5% surface solubility for iron and an iron content of 3.5% by weight. Other forcings were all from late 20th century NCEP-NCAR climatology to isolate the effects of N deposition [*Large and Yeager*, 2004].

[14] Atmospheric inputs of inorganic nitrogen to oceans during 1990s were obtained from University of California Irvine Chemical Transport Model (UCICTM) simulations with an embedded inorganic aerosol thermodynamic equilibrium model [*Luo et al.*, 2007]. The organic aerosols are not yet represented in the model owing to their complexity. Observations of nitrate (NO_3^-) and ammonium (NH_4^+) aerosols at North American sites compare well with UCICTM simulations by *Luo et al.* [2007]. Observations at European sites did not compare as well with those obtained from the model. Partitioning gas-phase precursors among modeled inorganic aerosol species and representing ammonia chem-

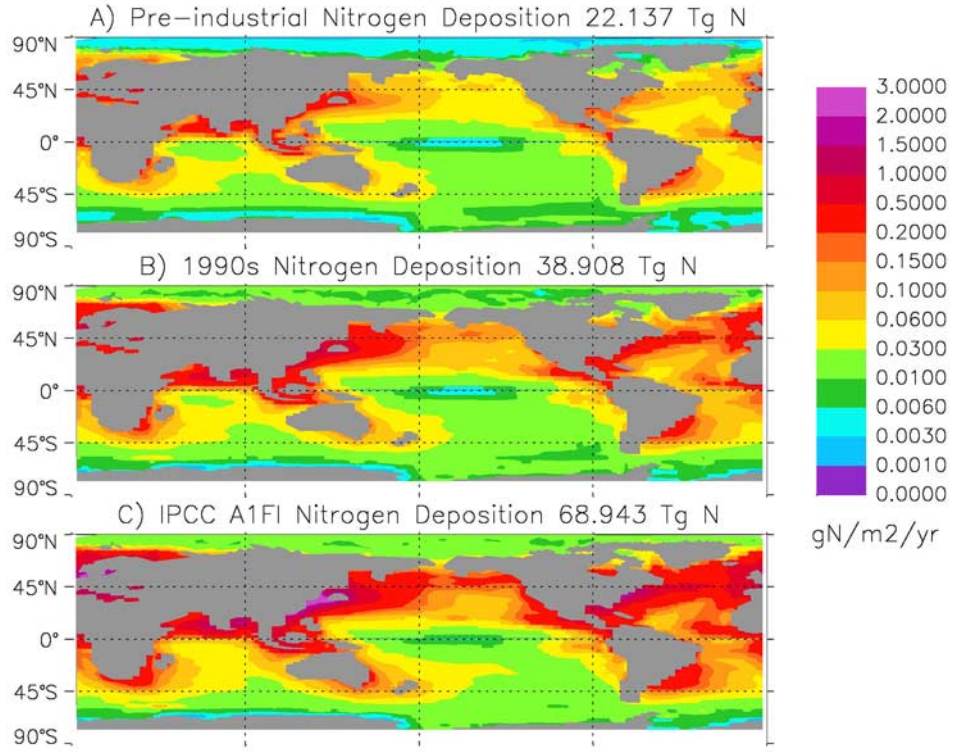

Figure 1. Spatial distribution of global oceanic nitrogen deposition for the Pre-industrial, 1990s, and IPCC-A1FI cases from the final year of simulations (year 64).

istry in the aerosol equilibrium model improved the simulated nitrate concentrations. On a global scale, inclusion of dust and sea salt aerosols resulted in better estimations of nitrate and ammonium concentrations over oceans, industrial regions and very dusty regions of North Africa. Ammonium and nitrate emissions during 1990s increased by a factor of two since Pre-industrial conditions, owing to increased anthropogenic impact in the present era on NO_3^- and NH_4^+ emissions [*Luo et al.*, 2007]. Here only the net land-to-sea nitrogen fluxes were considered and atmospheric inorganic nitrogen deposition was estimated by excluding oceanic ammonia emissions. The inorganic nitrogen deposition data were combined as nitrate and ammonia such that all forms of nitrogen oxide were classified as nitrate source to ocean and compounds that had nitrogen and hydrogen were grouped as ammonium source to ocean, assuming relatively rapid conversion within the oceans.

[15] The Pre-industrial and IPCC inorganic nitrogen deposition estimates were obtained as part of sensitivity studies. The winds in these simulations as well as those used to estimate emissions in 1990s were based on National Centers for Environment Prediction (NCEP) driven winds for the current era. These winds are better constrained by observations and perhaps more accurate than using model-derived winds for other time periods. In the Pre-industrial simulations, sources of CO, SO_x, NO_x, CH_4, and ammonia due to fertilizer use, fossil fuel combustion, and human induced ammonia emissions were excluded. In the IPCC runs CO, SO_x, NO_x and CH_4 emissions were scaled on the basis of IPCC-A1FI suggested values while retaining the 1990s spatial distributions. The emissions data were obtained from the IPCC emission scenario report for policy makers [*Intergovernmental Panel on Climate Change*, 2000].

3. Results

[16] Ocean biogeochemical cycling was simulated for 64 years with the three different nitrogen deposition forcings (shown in Figure 1). In order to assess the impact of low (Pre-industrial), intermediate (during 1990s) and high (IPCC-A1FI) atmospheric nitrogen deposition on marine ecosystem, the growth limitation factors for three phytoplankton groups, namely diatoms, small phytoplankton and diazotrophs were examined. Spatial distributions were obtained for the final year (year 64) of the simulation for each deposition case. During Pre-industrial N inputs, nutrient and light limitation factors reducing diatom growth (Figure 2a) were such that, ~36% of ocean area was nitrogen limited. As the inorganic N deposition increased from Pre-industrial values (low) to that in 1990s, and IPCC-A1FI, the regions which were nitrogen limited decreased to ~34% and ~30% respectively (Table 2). In these areas, the factor most limiting growth was shifted to other nutrients or light limitation (Table 2). For example, in the IPCC-A1FI case the percent of ocean area where iron limited growth increased by 1.5% (+1.2% for Si, +2.5% for P, and +0.6% for light, Table 2).

[17] Under the Pre-industrial N deposition, for the small phytoplankton (Figure 2b), 41% of the global ocean was nitrogen limited, 39% was iron limited, 9% was phosphorus limited and 11% was light limited. As N deposition increased from Pre-industrial conditions to 1990s, and IPCC-

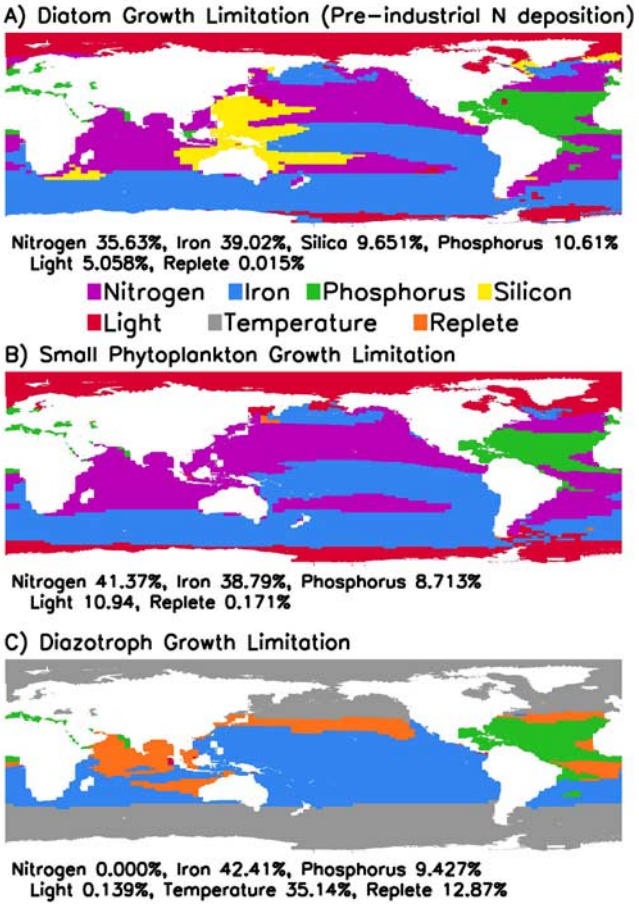

Figure 2. Factor most limiting growth rates for diatom, small phytoplankton, and diazotroph under Pre-industrial atmospheric N deposition from the final year of simulations (year 64).

A1FI, globally, there was a decrease in nitrogen limited regions by 1%, and 4% respectively, with increase mainly in Fe and P limited areas (Table 2). Comparing the diazotroph growth under Pre-industrial N deposition (Figure 2c), with that under N deposition in 1990s, and IPCC-AIF1, there was an increase in Fe and P limited regions across the global oceans (Table 2). Globally, since there was a decrease in N limitation for diatoms and small phytoplankton, they competed with the diazotrophs for available iron and phosphorus more efficiently. This resulted in a decrease in N fixation, as diazotroph growth was reduced under increased iron and phosphorus stress.

[18] The response of marine ecosystem to increased atmospheric N inputs can be accessed by calculating the differences between nitrogen fixation, sinking POC export and sea-air CO_2 exchange under various atmospheric nitrogen input conditions. Nitrogen deposition (Figures 3a and 4a) increased primarily over downwind regions off of the Asian, African, North and South American and Australian continents. There was a significant decrease in nitrogen fixation (Figures 3b and 4b) throughout the tropics and subtropics. Nitrogen fixation decreased strongly in north Indian Ocean, Bay of Bengal and Arabian Sea. This was due to reduction in diazotroph growth compared to diatoms and small phytoplankton which benefited from increased inorganic nitrogen deposition conditions. Nitrogen fixation did not decline in the equatorial Pacific (strongly Fe-limited) and in the Sargasso Sea (strongly P-limited).

[19] The sinking POC export (Figures 3c and 4c) at the depth of 103m correlated with sea-air CO_2 flux (Figures 3d and 4d) such that higher export corresponded to lower sea to air CO_2 flux. The POC export increased modestly with the increase in N deposition from Pre-industrial conditions especially at northern Pacific and Atlantic regions. They were highest for IPCC-A1FI scenario particularly at the north Indian Ocean region and off the coast of east Asia. The oceanic uptake of atmospheric CO_2 increased slightly across much of the globe excluding the Southern Ocean. The sea to air CO_2 flux increased in the Southern Ocean and subarctic North Pacific associated with the upwelling of inorganic carbon enriched waters as a result of increased export in ''upstream'' waters.

[20] Primary production and export increase while N fixation and atmospheric pCO_2 decrease as the atmospheric inorganic N deposition increased. Globally, the potential contribution of atmospheric N deposition to sinking Particulate Organic Nitrogen (PON) (Figure 5) at 103 m for the final year of simulation (year 64) increased over a wide area as deposition increased since Pre-industrial conditions. The high fractions in the subtropical North Atlantic and Arctic oceans reflect mainly very low export production in those regions. In the N-limited regions (Figure 2) atmospheric nitrogen deposition is directly increasing export by the fractions shown in Figure 5. The percent of export production supported by the three atmospheric N depositions (Figure 5) for the Arabian Sea was 8%, 13.5%, and 20.5% and for the Bay of Bengal regions was 14%, 23%, and 36.4%. In the western subtropical Pacific, between 26°N,119°E and 32°N,130°E the atmospheric N deposition

Table 2. Net Oceanic N Deposition (Tg N/year), Primary Production (Gt C/year), N Fixation (Tg N/year), Sinking POC (Gt C/year) for Year 64, Atmospheric pCO_2 (ppm/year) at the end of the 64 Year Simulations, Diatom, Small Phytoplankton and Diazotroph Nutrient and Light Limitation Factors Over Global Ocean Area

	Pre-Industrial	1990s	IPCC-A1FI
Oceanic N deposition	22.14	38.91 (+16.77)	68.94 (+46.8)
Total primary production	48.09	48.50 (+0.41)	49.07 (+0.98)
Total nitrogen fixation	143.45	139.15 (−4.3)	132.15 (−11.3)
Total sinking POC	5.79	5.86 (+0.07)	5.95 (+0.16)
Final atmospheric PCO_2	276.50	275.87 (−0.63)	274.84 (−1.66)
Diatoms			
N-limited	35.63%	33.68% (−1.95)	29.78% (−5.85)
Fe-limited	39.02%	39.7% (+0.68)	40.56% (+1.54)
P-limited	10.61%	11.39% (+0.78)	13.11% (+2.5)
Si-limited	9.65%	9.95% (+0.3)	10.84% (+1.19)
Light limited	5.06%	5.24% (+0.2)	5.67% (+0.61)
Small Phytoplankton			
N-limited	41.37%	40.15% (−1.22)	37.41% (−3.96)
Fe-limited	38.79%	39.29% (+0.5)	40.59% (+1.8)
P-limited	8.71%	9.36% (+0.65)	10.9% (+2.19)
Light limited	10.94%	10.98% (+0.04)	10.88% (−0.06)
Diazotrophs			
Fe-limited	42.41%	42.56% (+0.15)	43.03% (+0.89)
P-limited	9.43%	10.01% (+0.58)	11.43% (+2.0)
Light limited	0.14%	0.12% (+0.02)	0.11% (+0.03)

Value in parenthesis in columns 3 and 4 shows the difference of these values relative to Pre-industrial conditions.

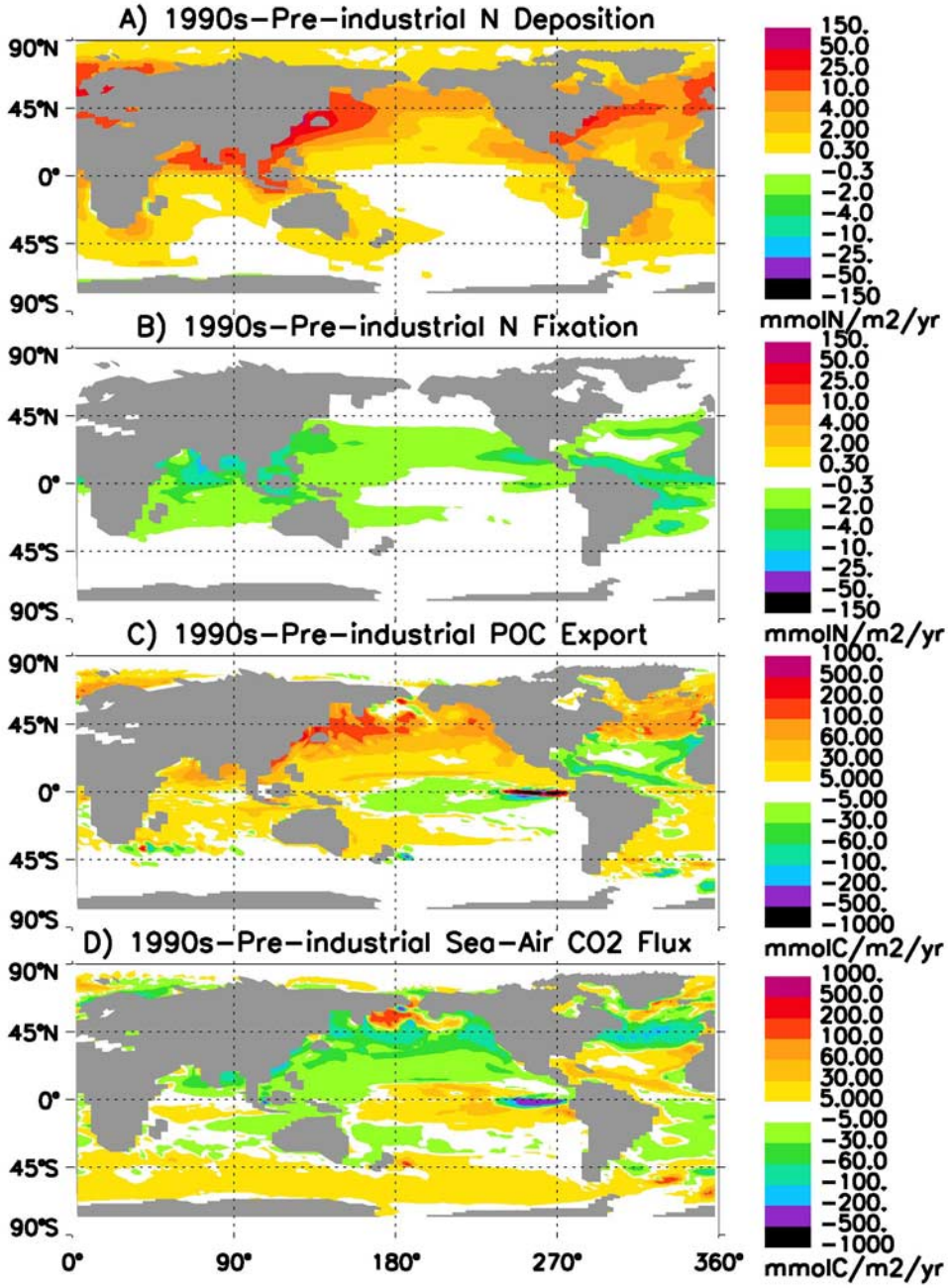

Figure 3. Change in inorganic nitrogen forcing and the ocean biogeochemical responses are shown for the 1990s with respect to Pre-industrial conditions. Each plot shows the difference between 1990s and Pre-industrial results.

supported export was 9%, 27%, and 56% for Pre-industrial, 1990s, and IPCC-A1FI conditions, respectively. The export fractions also increased in the open ocean regions of North Pacific Ocean from <3% during Pre-industrial conditions to nearly 10% under IPCC-A1FI nitrogen deposition scenario (Figure 5).

[21] The net nitrogen inputs via wet and dry deposition across the Arabian Sea region were estimated to be 0.32 gN/m^2/year by *Bange et al.* [2000]. The atmospheric inputs of inorganic nitrogen for this region from our global simulations with N deposition conditions during the 1990s were 0.46 gN/m^2/year [*Luo et al.*, 2007]. The maximum increase in sinking POC export of 0.16 Gt C/year was obtained for the maximum increase in atmospheric nitrogen deposition of 47 Tg N/year since Pre-industrial conditions for the IPCC-A1FI case. This simulation had the maximum global increase in primary production of 0.98 Gt C/year and the maximum decrease in atmospheric pCO_2 of 1.66 ppm relative to the Pre-industrial control (Figure 4 and Table 2).

[22] In reality, atmospheric N inputs to oceans are transient and deposition varies, but our simulations employ a constant atmospheric N deposition per year for 64 years. Thus, by focusing on year 64, we report only the perturbations in ocean biogeochemical cycling that are sustainable over decadal timescales. There is an initial stronger response that declines over time (Figure 6). Changes in

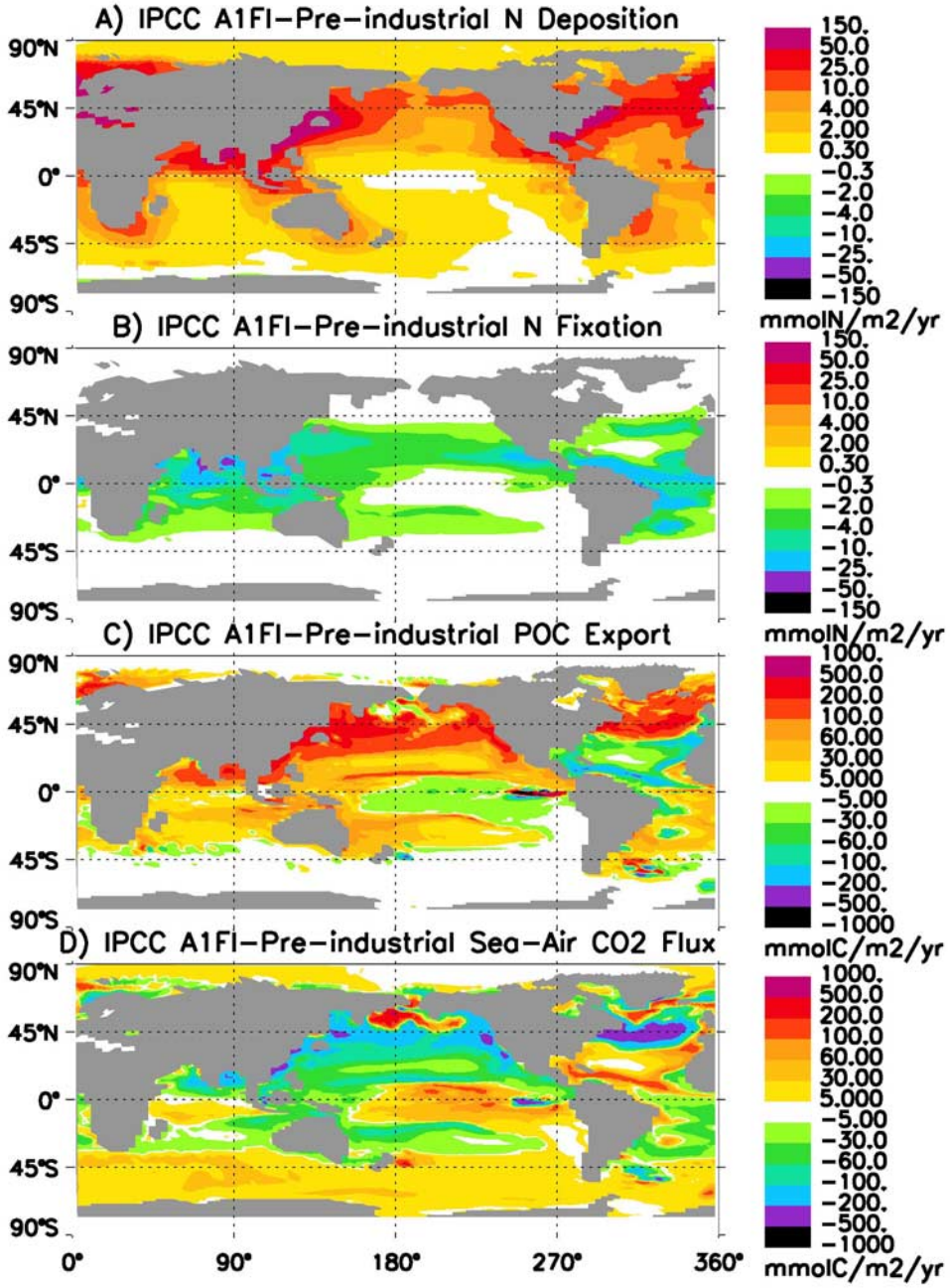

Figure 4. Change in inorganic nitrogen forcing and the ocean biogeochemical responses are shown for the IPCC-A1FI with respect to Pre-industrial conditions. Each plot shows the difference between IPCC-A1FI and Pre-industrial results.

sea to air CO_2 and O_2 fluxes over the 64 years were negligible for Pre-industrial N deposition case with mean fluxes of 0.0025 Pg C/year and 2 Tmol O_2/year respectively. There was a steep increase in atmospheric CO_2 uptake during the first few years of the IPCC-A1FI nitrogen deposition case (Figure 6). This declined and leveled off during the latter half of the simulations as a result of reductions in primary production due to an increase in iron and phosphorus limitation for the phytoplankton in previously N limited regions. The sea to air O_2 fluxes (Figure 6) concurred with the sea to air CO_2 flux trends such that the initial increase in phytoplankton production associated with increased N deposition for the IPCC-A1FI case resulted in higher oxygen outgassing followed by a decline and leveling off during the final 30 years of simulation. Note that significant perturbations in air-sea gas exchange are still seen after 64 years in each simulation, relative to Pre-industrial case.

4. Discussion

[23] On a global scale the effects of increased atmospheric inorganic nitrogen deposition on the carbon cycle were modest. The regional effects of increased atmospheric inorganic nitrogen loading were however, quite significant

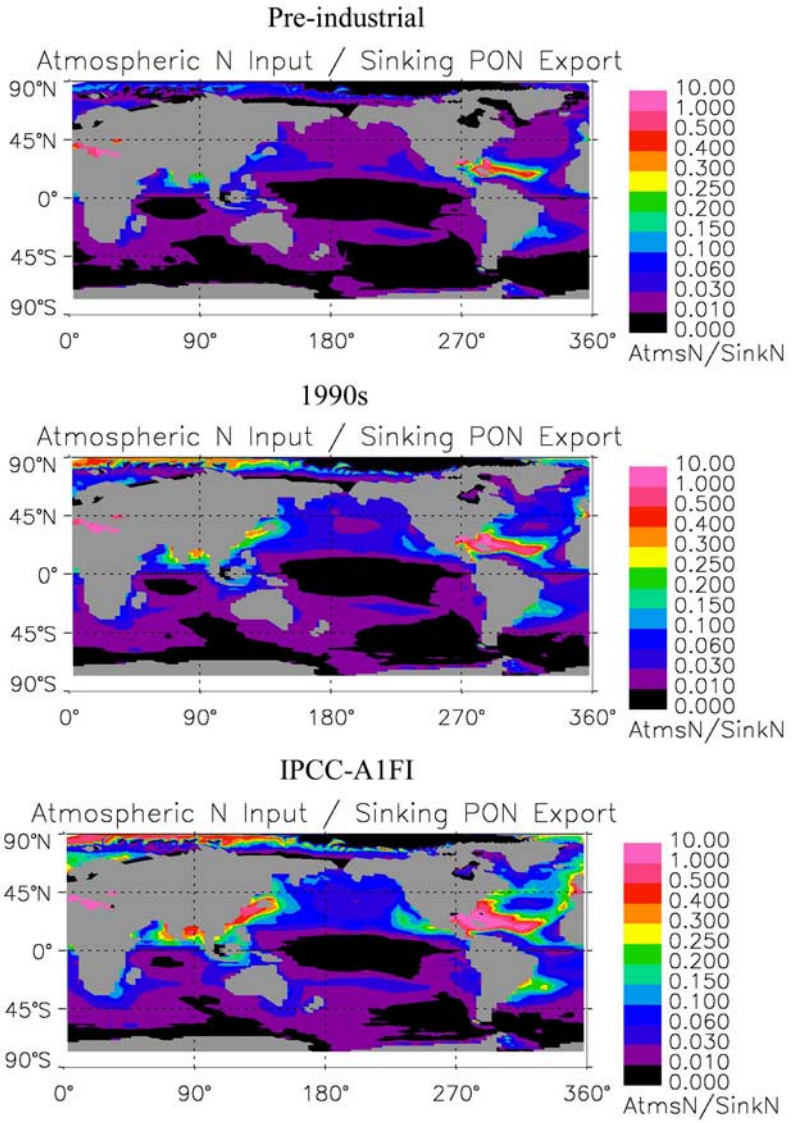

Figure 5. Global distribution of the ratio between atmospheric N input and sinking PON export at 103 m for Pre-industrial, 1990s, and IPCC-A1FI cases from the final year of simulations (year 64).

such as off the coast of Asia and eastern coast of North America. Regions which were nitrogen limited prior to increased atmospheric inorganic nitrogen inputs become less N stressed after N additions, resulting in increased export production and oceanic uptake of CO_2. As the deposition increased in our simulations from Pre-industrial levels, small phytoplankton and diatoms grow more efficiently relative to diazotrophs in N-limited regions. As P and Fe get increasingly depleted at higher N deposition, the diazotrophs become more P or Fe stressed, reducing N fixation.

[24] The decrease in oceanic N fixation partially compensates for the increase in atmospheric N inputs. Comparing the increase of ~17 Tg N by atmospheric inputs during 1990s since Pre-industrial conditions, with the N fixation decrease by ~4 Tg N (Table 2). The reduction in N fixation reduced the total increase in new N inputs to surface waters from atmospheric deposition by ~24%. The total new nitrogen inputs into the ocean as a result of increased N deposition during IPCC-A1FI scenarios were reduced by 23% respectively owing to decreased N fixation. Increasing N deposition raises the inorganic N/P ratios in surface waters reducing the competitiveness of the diazotrophs [*Moore and Doney*, 2007].

[25] Since, nitrogen is limiting in the oligotrophic regions of subtropical North Atlantic and Pacific, the net effect of primary production is to export surface nitrogen to the deep as sinking biogenic particles [*Hansell and Feely*, 2000]. This is also apparent in our simulations (Figure 5), as the nitrogen limited subtropical North Atlantic and Pacific regions with increased atmospheric N inputs had increased sinking particulate organic matter export.

[26] Increasing N inputs in the Arabian Sea and Bay of Bengal could imply a shift toward enhanced P limitation for small phytoplankton and diatoms. This is prevented by the high rates of water column denitrification in these areas that result in low surface water N/P ratios [*Moore and Doney*, 2007]. Increased P limitation is also inhibited by stronger water column denitrification the Pacific basin [*Codispoti et*

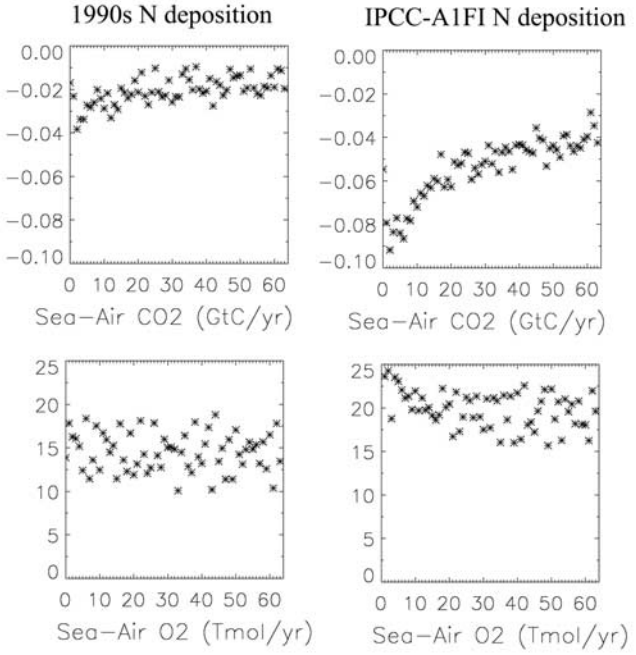

Figure 6. Trends in sea to air CO_2 and O_2 fluxes during the 64 years for the 1990s, and IPCC-A1FI, nitrogen deposition scenarios

al., 2001; *Moore and Doney*, 2007]. Hence increasing atmospheric nitrogen inputs to regions with low surface water N/P ratios could steadily increase export production and uptake of atmospheric CO_2.

[27] Our results demonstrate the sensitivity of marine biogeochemical cycling to variations in atmospheric N deposition. The cumulative impacts since Pre-industrial era and through the 21st century will be addressed with transient simulations in the future. Our current study shows that although globally the effect of anthropogenically increased atmospheric nitrogen inputs may be modest, the regional impacts are significant. The anthropogenic perturbation in N deposition should be viewed in the context of other anthropogenic modifications of the biogeochemical cycles that are increasing riverine nutrient transport [*Smith et al.*, 2003] and possibly increasing atmospheric deposition of organic nitrogen [*Cornell et al.*, 1995] and other bioavailable nutrients such as P and Fe [*Luo et al.*, 2005; *Fan et al.*, 2006]. Combined these perturbations may have a significant effect on atmospheric pCO_2 and hence Earth's climate.

[28] **Acknowledgments.** We thank Huisheng Bian for help with the UCICTM. This work was supported by funding from NSF grant OCE-0452972 to Moore and Zender. Computations supported by the Earth System Modeling Facility at UCI (NSF ATM- O321380) and by the Climate Simulation Laboratory at National Center for Atmospheric Research. The National Center for Atmospheric Research is sponsored by the U.S. National Science Foundation.

References

Bange, H. W., T. Rixen, A. M. Johansen, R. L. Siefert, R. Ramesh, V. Ittekkot, M. R. Hoffmann, and M. O. Andreae (2000), A revised nitrogen budget for the Arabian Sea, *Global Biogeochem. Cycles*, *14*(4), 1283–1297.

Codispoti, L. A., J. A. Brandes, J. P. Christensen, A. H. Devol, S. W. A. Naqvi, H. W. Paerl, and T. Yoshinari (2001), The oceanic fixed nitrogen and nitrous oxide budgets: Moving targets as we enter the anthropocene?, *Sci. Mar.*, *65*(Suppl.), 85–105.

Collins, W. D., et al. (2006), The Community Climate System Model version 3 (CCSM3), *J. Clim.*, *19*(11), 2122–2143.

Cornell, S., A. Rendell, and T. Jickells (1995), Atmospheric inputs of dissolved organic nitrogen to the oceans, *Nature*, *376*, 243–246.

Crutzen, P. J. (1990), Biomass burning: A large factor in the photochemistry and ecology of the tropics, paper presented at Chapman Conference on Global Biomass Burning: Atmospheric, Climate and Biospheric Implications, AGU, Williamsburg, Va.

De Leeuw, G., et al. (2001), Atmospheric input of nitrogen into the North Sea: ANICE project overview, *Cont. Shelf Res.*, *21*, 2073–2094.

Doney, S. C., K. Lindsay, and J. K. Moore (2003), Global ocean carbon cycle modeling, in *Ocean Biogeochemistry: A JGOFS Synthesis*, edited by M. Fashom, pp. 217–238, Springer, New York.

Doney, S. C., et al. (2004), Evaluating global ocean carbon models: The importance of realistic physics, *Global Biogeochem. Cycles*, *18*, GB3017, doi:10.1029/2003GB002150.

Doney, S. C., K. Lindsay, I. Fung, and J. John (2006), Natural variability in a stable, 1000-yr global coupled climate-carbon cycle simulation, *J. Clim.*, *19*(13), 3033–3054.

Duce, R. A. (1986), The impact of atmospheric nitrogen, phosphorous, and iron species on marine biological productivity, in *The Role of Air-Sea Exchange in Geochemical Cycling*, edited by P. Buat-Menard, pp. 497–529, Springer, New York.

Duce, R. A., et al. (1991), The atmospheric input of trace species to the world ocean, *Global Biogeochem. Cycles*, *5*(3), 193–259.

Fan, S. M., W. J. Moxim, and H. Levy II (2006), Aeolian input of bioavailable iron to the ocean, *Geophys. Res. Lett.*, *33*, L07602, doi:10.1029/2005GL024852.

Galloway, J. N. (1995), Acid deposition: Perspectives in time and space, *Water Air Soil Pollut.*, *85*(1), 15–24.

Galloway, J. N., and E. B. Cowling (2002), Reactive nitrogen and the world: 200 years of change, *Ambio*, *31*, 64–71.

Geider, R. J., H. L. MacIntyre, and T. M. Kana (1998), A dynamic regulatory model of phytoplankton acclimation to light, nutrients, and temperature, *Limnol. Oceanogr.*, *43*, 679–694.

Gruber, N. (2004), The dynamics of the marine nitrogen cycle and its influences on atmospheric CO_2 variations, in *The Ocean Carbon Cycle and Climate*, edited by M. Follows and T. Oguz, pp. 97–148, Springer, New York.

Hameed, S., and J. Dignon (1988), Changes in the geographical distributions of global emissions of NO_X and SO_X from fossil-fuel combustion between 1966 and 1980, *Atmos. Environ.*, *22*, 441–449.

Hansell, D. A., and R. A. Feely (2000), Atmospheric intertropical convergence impacts surface ocean carbon and nitrogen biogeochemistry in the western tropical Pacific, *Geophys. Res. Lett.*, *27*(7), 1013–1016.

Intergovernmental Panel on Climate Change (2000), *Special Report on Emission Scenarios*, edited by N. Nakicenovic et al., 599 pp., Cambridge Univ. Press, New York.

Jassby, A. D., J. E. Reuter, R. P. Axler, C. R. Goldman, and S. H. Hackley (1994), Atmospheric deposition of nitrogen and phosphorus in the annual nutrient load of Lake Tahoe (California-Nevada), *Water Resour. Res.*, *30*(7), 2207–2216.

Jickells, T. D. (1998), Nutrient biogeochemistry of the coastal zone, *Science*, *281*, 217–222.

Jickells, T. (2002), Emissions from the oceans to the atmosphere, deposition from the atmosphere to the oceans and the interactions between them, in *Challenges of a Changing Earth*, edited by W. Steffen et al., pp. 93–96, Springer, New York.

Jickells, T. D. (2005), External inputs as a contributor to eutrophication problems, *J. Sea Res.*, *54*, 58–69.

Large, W. G., and S. G. Yeager (2004), Diurnal to decadal global forcing for ocean and sea-ice models: The data sets and flux climatologies, *NCAR Tech. Note NCAR/TN-460+STR*, 111 pp., Natl. Cent. for Atmos. Res., Boulder, Colo.

Logan, J. A. (1983), Nitrogen oxides in the troposphere: Global and regional budgets, *J. Geophys. Res.*, *88*, 10,785–10,807.

Luo, C., N. M. Mahowald, N. Meskhidze, Y. Chen, R. L. Siefert, A. R. Baker, and A. M. Johansen (2005), Estimation of iron solubility from observations and a global aerosol model, *J. Geophys. Res.*, *110*, D23307, doi:10.1029/2005JD006059.

Luo, C., C. S. Zender, H. Bian, and S. Metzger (2007), Role of ammonia chemistry and coarse mode aerosols in global climatological inorganic aerosol distributions, *Atmos. Environ.*, *41*, 2510–2533.

Moore, J. K., and S. C. Doney (2007), Iron availability limits the ocean nitrogen inventory stabilizing feedbacks between marine denitrification and nitrogen fixation, *Global Biogeochem. Cycles*, *21*, GB2001, doi:10.1029/2006GB002762.

Moore, J. K., S. C. Doney, J. C. Kleypas, D. M. Glover, and I. Y. Fung (2002), An intermediate complexity marine ecosystem model for the global domain, *Deep Sea Res., Part II*, *49*, 403–462.

Moore, J. K., S. C. Doney, and K. Lindsay (2004), Upper ocean ecosystem dynamics and iron cycling in a global three-dimensional model, *Global Biogeochem. Cycles*, *18*, GB4028, doi:10.1029/2004GB002220.

Moore, J. K., S. C. Doney, K. Lindsay, N. Mahowald, and A. F. Michaels (2006), Nitrogen fixation amplifies the ocean biogeochemical response to decadal timescale variations in mineral dust deposition, *Tellus, Ser. B*, *58*, 560–572.

Nixon, S. W. (1995), Coastal marine eutrophication—A definition, social causes, and future concerns, *Ophelia*, *41*, 199–219.

Paerl, H. W. (1985), Enhancement of marine primary productivity by nitrogen enriched acid rain, *Nature*, *315*, 747–749.

Paerl, H. W. (1993), Emerging role of atmospheric nitrogen deposition in coastal eutrophication—Biogeochemical and trophic perspectives, *Can. J. Fish. Aquat. Sci.*, *50*(10), 2254–2269.

Paerl, H. W. (1995), Coastal eutrophication in relation to atmospheric nitrogen deposition—Current perspectives, *Ophelia*, *41*, 237–259.

Paerl, H. W., and D. R. Whittal (1999), Anthropogenically-derived atmospheric nitrogen deposition, marine eutrophication and harmful algal bloom expansion: Is there a link?, *Ambio*, *28*, 307–311.

Paerl, H. W., R. L. Dennis, and D. R. Whitall (2002), Atmospheric deposition of nitrogen: Implications for nutrient over-enrichment of coastal waters, *Estuaries*, *25*, 677–693.

Prospero, J. M., K. Barrett, T. Church, F. Dentener, R. A. Duce, J. N. Galloway, H. Levy, J. Moody, and P. Quinn (1996), Atmospheric deposition of nutrients to the North Atlantic, *Biogeochemistry*, *35*, 27–73.

Pryor, S. C., and L. L. Sorensen (2002), Dry deposition of reactive nitrogen to marine environments: Recent advances and remaining uncertainties, *Mar. Pollut. Bull.*, *44*, 1336–1340.

Smith, S. V., et al. (2003), Humans, hydrology, and the distribution of inorganic nutrient loading to the ocean, *Bioscience*, *53*(3), 235–245.

Spokes, L. J., S. G. Yeatman, S. H. Cornell, and T. D. Jickells (2000), Nitrogen deposition to the eastern Atlantic Ocean: The importance of south-easterly flow, *Tellus, Ser. B*, *52*, 37–49.

Van Mooy, B. A. S., R. G. Keil, and A. H. Devol (2002), Impact of suboxia on sinking particulate organic carbon: Enhanced carbon flux and preferential degradation of amino acids via denitrification, *Geochim. Cosmochim. Acta*, *66*(3), 457–465.

Warneck, P. (1988), *Chemistry of the Natural Atmosphere*, 757 pp., Elsevier, New York.

Yeager, S. G., W. G. Large, J. J. Hack, and C. A. Shields (2006), The low-resolution CCSM3, *J. Clim.*, *19*(11), 2545–2566.

Zender, C. S., H. Bian, and D. Newman (2003), The Mineral Dust Entrainment and Deposition (DEAD) model: Description and 990s dust climatology, *J. Geophys. Res.*, *108*(D14), 4416, doi:10.1029/2002JD002775.

A. Krishnamurthy, C. Luo, J. K. Moore, and C. Z. Zender, Earth System Science Department, University of California, Irvine, CA 92697, USA. (aparnak@uci.edu)